7-21

Macromodel for micromechanical, multi-electrode structures in force feedback control systems

M. Handtmann, R. Aigner, F. Plötz, G. Wachutka*

Infineon Corporate Research, Otto-Hahn-Ring 6, D-81730 Munich, Germany
*Institute for Physics of Electrotechnology, Munich University of Technology, Arcisstr. 21, D-80290 Munich, Germany

Abstract

Electrostatic force feedback loops are commonly used for measurement and position control in micromechanical sensors and actuators. They are widely implemented with switched capacitor, sigma-delta(Σ/Δ) architectures as they provide perfect compatibility with capacitive sensing methods. The electromechanical subsystem, as a vital part of a Σ/Δ-loop, strongly influences the loop characteristics. In order to characterize a Σ/Δ-loop, however, transient simulations over a long time period are inevitable. Full 3-D physical simulations (FEM/BEM) at system level are numerically impractical. Therefore, effective macromodels of the electro-mechanical subsystem are required. Established macromodels can handle one-dimensional systems and weakly coupled multi-dimensional systems but are not applicable to multidimensional, multi-electrode systems [1,2,3]. A novel modeling technique is presented for micromechanical, multi-electrode structures which is based on Lagrange's equations. It considers the coupling of the structure kinematics with the electrical field between the electrodes. It further reflects parasitic excitation of the mechanical fundamental eigenmodes of the structure. The technique is applied to a new electrostatic levitation system controlling a micromechanical plate.

1. Introduction

Fig. 1 shows an example of a conducting moveable plate situated between two sets of eight fixed electrodes. If voltages are applied to the electrodes, electrostatic forces are generated which are capable of balancing inertial forces and, therefore, bringing the plate into the desired position. Using the same electrode arrangement allows capacitive sensing of the two tilting degrees of freedom and the vertical translation of the plate. Hence, appropriate adjustment of the forces, i.e. control of the electrode voltages as a function of the position of the plate, allows stable levitation of the plate.

State-of-the-art capacitive sensing is realized with a CMOS switched capacitor circuit which naturally leads to time-multiplexed sensing and feedback at high frequencies. Often, through quantization of the feedback force, a Σ/Δ-structure is obtained where the mechanical elements act as the required low pass filter [2]. Therefore, the plate is subjected to forces which have a broadband frequency spectrum and thus can excite eigenmodes. By refining the electrode structures, it becomes possible to sense and control these modes. In fact, in the structure shown the first bending mode can be controlled.

Design and characterization of stable position control and measurement systems in Σ/Δ-architecture require models which describe the kinematics of the mechanical system including the first eigenmodes which lie in the frequency band of interest. With a view to proving the system stability and analyzing its performance, it is crucial to model the system-inherent non-linearity and cross-coupling effects. On the other hand, since Σ/Δ-modulation is a frequency based technique (noise shaping), long transient simulations are required to verify the effects of the mechanical subsystem on the inherent signal processing. In other words, a method is required which extracts behavioral macromodels allowing for of simulation at system level.

2. Theory

The method presented here belongs to the basic-function methods [4] and is based on Lagrange's equations [5]

$$\frac{d}{dt}\left(\frac{\partial T}{\partial \dot{q}_v}\right) - \frac{\partial T}{\partial q_v} + \frac{\partial E_{pot}}{\partial q_v} = 0$$

where T denotes the kinetic energy, E_{pot} the potential energy, q_v the generalized coordinates, $\dot{q}_v = \frac{dq_v}{dt}$ the generalized velocities and t the time.

These equations imply that the possible motions of the mechanical structure are described by a set of discrete generalized coordinates q_v. Therefore, from an infinite number of degrees of freedom associated with the continuously deformable structure, a limited number of motion configurations have to be selected and related to the generalized coordinates. Hence, using the Lagrange equations restricts the possible shape and position of the mechanical structure.

In the case of a flexible moveable disk, the appropriate choice for a set of motion configurations is the six degrees of freedom which represent the rigid body motions of the undeformed structure and, additionally, the amplitudes of the eigenmodes of interest. While this choice is sufficient for a floating structure, the rigid body position of a flexible suspended structure may be overconstrained, where the suspension is understood as mechanical coupling to further mechanical structures, described by a force/displacement pair. Hence, further deformation shapes have to be defined to

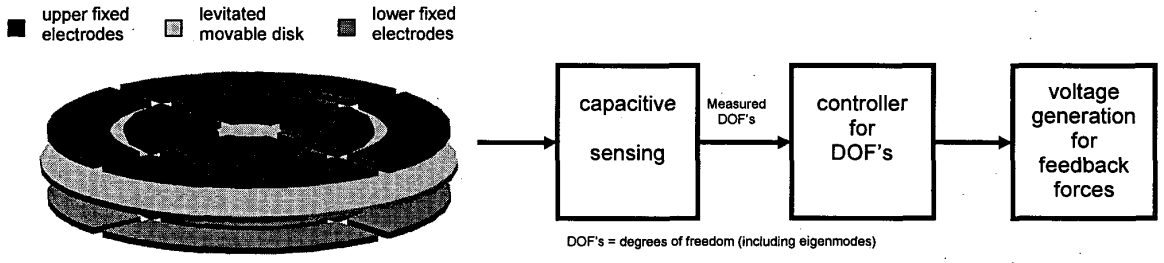

Fig. 1: A micromechanical, multi-electrode system for levitation of a conducting moveable plate situated between two sets of electrodes.

associate a rigid body position and a appropriate deformation with each possible displacement configuration at the suspension points. It is practicable to use this displacements configurations $\vec{\mathbf{u}}_{sus}$ as the first subset of the generalized coordinates q_V and the amplitudes m_i of the eigenmodes as the remaining ones. The displacement $\vec{\mathbf{u}}$ at the location $\vec{\mathbf{x}}$ of the undeformed structure can be described by

$$\vec{\mathbf{u}}(\vec{\mathbf{x}}) = \vec{\mathbf{x}}_B(\vec{\mathbf{u}}_{sus}) + \underline{\mathbf{D}}(\vec{\mathbf{u}}_{sus})\left[\vec{\mathbf{x}} + \vec{\mathbf{g}}(\vec{\mathbf{u}}_{sus}, \vec{\mathbf{x}}) + \underline{\mathbf{G}}(\vec{\mathbf{u}}_{sus}, \vec{\mathbf{x}})\vec{\mathbf{m}}\right]$$

where $\vec{\mathbf{x}}_B$ denotes the translation of the basis point of the undeformed structure, $\underline{\mathbf{D}}$ the rotation of the undeformed structure with respect to the basis point $\vec{\mathbf{x}}_B$, $\vec{\mathbf{g}}$ the deformation shapes, due to a overconstrained suspension, and $\underline{\mathbf{G}}$ the deformation due to the eigenmodes.

Since the eigenmode representation is based on a linearized system, it is suggestive to linearize the deformations shapes and eigenmodes with respect to the undeformed structure. Then, the structures deformation is notated in a separated formulation $\underline{\mathbf{G}}'[\vec{\mathbf{u}}_{sus} \quad \vec{\mathbf{m}}]^T$. As only small deformations are expected in most applications, the material can be assumed linear and the error introduced thereby neglected. For non-linear material a partial correction occurs, since the inner potential energy, which is related to the nonlinear stiffness of the material and inserted in the Lagrange equations, is still correct for a given deformation.

The eigenmode shapes $\underline{\mathbf{G}}$ are obtained analytically or by FEM simulation from the usual separation formulation under the condition that the suspension displacements are held at zero. For a structure with an underconstrained suspension, undefined degrees of freedom for the rigid body modes exist, which require further side conditions. Setting the integral of these free body motions over the structures volume to zero is practicable, since this decouples partially the rigid body motions from the eigenmodes.

Even if the eigenmodes are likely to be close to the modes of the loaded system, they are not exactly identical to them. However, it would not be effective to take a certain load on the mechanical structure into consideration while determining the mode shapes, since the load depends on the state of the system and is therefore not predictable. This modeling error introduced thereby can be estimated from worst case analysis.

State of the art computing efficiency allows fast eigenmode analysis even for complex structures and, thus, for most practicable complete moveable structures. This definition describes structures whose suspension is fixed or the entire body is floating. The focus will be on this type of structures below. The displacement $\vec{\mathbf{u}}$ at the location $\vec{\mathbf{x}}$ reduces to

$$\vec{\mathbf{u}}(\vec{\mathbf{x}}) = \underline{\mathbf{G}}(\vec{\mathbf{x}})\vec{\mathbf{m}}$$

in the first case and

$$\vec{\mathbf{u}}(\vec{\mathbf{x}}) = \vec{\mathbf{x}}_S + \underline{\mathbf{D}}(\phi, \vartheta, \varphi)\left(\vec{\mathbf{x}} + \underline{\mathbf{G}}(\vec{\mathbf{x}})\vec{\mathbf{m}}\right)$$

in the second one, where $\vec{\mathbf{x}}_s$ stands for the motion of the center of mass and $\underline{\mathbf{D}}$ for the rotation of the undeformed body, described by the eulerian angles ϕ, ϑ, φ. Note that the first notation is included in the second one as a special case. Eigenmode extraction of the second case includes the constraint, that the center of mass and the rotations are fixed over the body's volume.

The kinetic energy T and potential energy E_{pot} are expressed as functions of the generalized coordinates. Preferably, the coordinates of the center of mass, the Eulerian angles and the amplitudes of the eigenmodes are chosen. Integration over the volume V of the structure describes the kinetic energy T

$$T = \frac{\rho}{2}\int_V \left(\vec{\mathbf{u}}^T\vec{\mathbf{u}}\right)dV$$

$$\vec{\mathbf{u}} = \vec{\mathbf{x}}_S + \dot{\underline{\mathbf{D}}}\left(\vec{\mathbf{x}} + \underline{\mathbf{G}}\vec{\mathbf{m}}\right) + \underline{\mathbf{D}}\underline{\mathbf{G}}\vec{\mathbf{m}} = \dot{\vec{\mathbf{x}}}_S + \underline{\mathbf{D}}\left(\vec{\omega}\times\left(\vec{\mathbf{x}} + \underline{\mathbf{G}}\vec{\mathbf{m}}\right) + \underline{\mathbf{G}}\vec{\mathbf{m}}\right)$$

where ρ denotes the density of mass of the structure and the dot differentiation with respect to time t. The notation using the rotation vector ω associated with the rotated coordinate system condenses the notation while performing the integration:

$$T = \frac{1}{2}M\left|\dot{\vec{x}}_s\right|^2 + \frac{1}{2}\vec{\omega}^T\underline{\theta}(\vec{\mathbf{m}})\vec{\omega} + \vec{\omega}^T\underline{\mathbf{A}}(\vec{\mathbf{m}})\dot{\vec{\mathbf{m}}} + \frac{1}{2}\dot{\vec{\mathbf{m}}}^T\underline{\mathbf{M}}\dot{\vec{\mathbf{m}}}$$

$$\underline{\theta}(\vec{\mathbf{m}}) = \underline{\theta}_{undef} + \rho\int_V\left[\underline{\mathbf{I}}_3\left(\vec{\mathbf{m}}^T\underline{\mathbf{G}}^T\vec{\mathbf{x}} + \vec{\mathbf{m}}^T\underline{\mathbf{G}}^T\underline{\mathbf{G}}\vec{\mathbf{m}}\right) - 2\vec{\mathbf{x}}\vec{\mathbf{m}}^T\underline{\mathbf{G}}^T - \underline{\mathbf{G}}\vec{\mathbf{m}}\vec{\mathbf{m}}^T\underline{\mathbf{G}}^T\right]dV$$

$$\underline{\mathbf{A}}(\vec{\mathbf{m}}) = \rho\int_V\left[\left(\vec{\mathbf{x}} + \underline{\mathbf{G}}\vec{\mathbf{m}}\right)\times\underline{\mathbf{G}}\right]dV;\quad \underline{\mathbf{M}} = \rho\int_V\underline{\mathbf{G}}^T\underline{\mathbf{G}}dV$$

The first term of the kinetic energy is associated with the rigid body translation, where M stands for the total mass of the structure. As the center of mass has been chosen as reference point, this term is decoupled from the remaining motion. The rigid body rotations occurs in the second term. The matrix of moment of inertia of the undeformed structure $\underline{\theta}_{undef}$ has to be corrected, due to the deformation. The integration required for the correction matrix needs to be performed on each element separately. The third term describes the coupling of the eigenmodes with the rotation of the rigid body. The cross product operation which occurs in the matrix A has to be used with respect to each column vector of G. The kinetic energy due to the eigenmodes is considered in the last term. The mass matrix $\underline{\mathbf{M}}$ can be obtained directly from a FEM model of the structure by multiplication of the mass matrix of the FEM model with the eigenvectors describing the eigenmodes.

Similarly, the matrix $\underline{\mathbf{A}}$ and the correction term in the matrix of moment of inertia $\underline{\theta}$ can be related to a FEM model of the structure. For this, the output of an FEM element has to be extended by terms of the form

$$\int_{V_{element}} g_i(\vec{\mathbf{x}})x_j dV_{element}$$

where g_i stands for a component of the elements form function and x_j for a component of the vector $\vec{x}$. Then, summation over the element outputs replaces the necessary integration. Furthermore, respecting the orthogonality of the eigenmodes and the constraints used for the eigenmode determination, simplifies these two matrices prior to integration.

The potential energy consists of two terms: the mechanical deformation energy $E_{pot,def}$ of the structure and the electrostatic energy $E_{pot,el}$ associated with the voltages applied to the electrodes.

The deformation energy $E_{pot,def}$ is of the form [6]

$$E_{pot,def} = \frac{1}{2}\vec{\mathbf{u}}_{FEM}^T\underline{\mathbf{K}}_{FEM}\vec{\mathbf{u}}_{FEM} = \frac{1}{2}\vec{\mathbf{m}}^T\underline{\mathbf{K}}\vec{\mathbf{m}}$$

$$\underline{\mathbf{K}}_{FEM} = \underline{\mathbf{K}}_E + \underline{\mathbf{S}}_E;\quad \underline{\mathbf{K}} = \underline{\mathbf{U}}_{Eigen}^T\underline{\mathbf{K}}_{FEM}\underline{\mathbf{U}}_{Eigen}$$

where $\underline{\mathbf{K}}_{FEM}$ is the total element stiffness matrix of the FEM model, consisting of the element stiffness matrix $\underline{\mathbf{K}}_E$ and the stress stiffness matrix $\underline{\mathbf{S}}_E$, and $\underline{\mathbf{K}}$ the eigenmode stiffness matrix, obtained by multiplication of the total element stiffness matrix with the eigenvector matrix $\underline{\mathbf{U}}_{Eigen}$. If the model shall includes non-linear material effects, the eigenmode stiffness matrix becomes a function of the amplitudes of the eigenmodes. To make simulation fast this function should be expressed in terms of analytical functions,

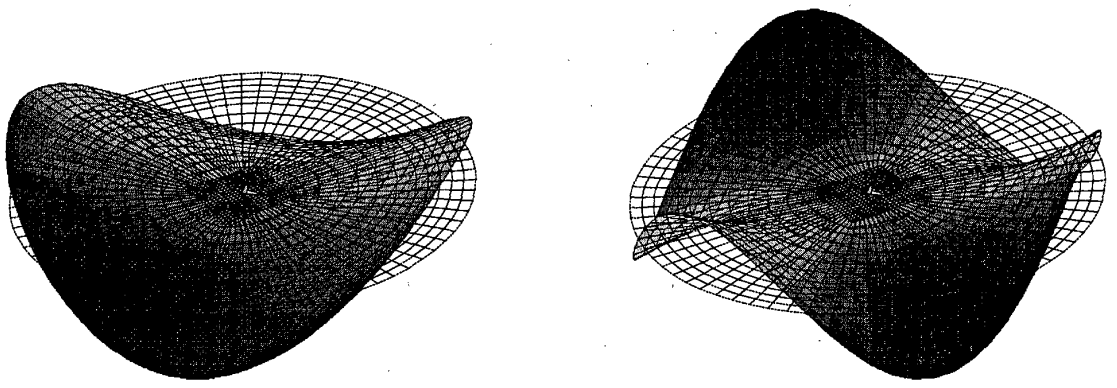

Fig. 2: modeshapes of 1st and 3rd considered eigenmode. the 2nd and 4th considered eigenmode is obtained by rotation of these two modes around the z-axis

obtained either from analytical methods or by fitting stiffness matrix data from FEM simulations.

The respective term in the Lagrange equations related to the electrical potential energy can be expressed as [1]:

$$\frac{\partial E_{pot,el}}{\partial q_v} = F_E = \frac{1}{2} V^T \frac{d[C_{ij}]}{dq_v} V$$

where C_{ij} is the capacitance matrix of the multi-electrode structure and V is a column vector consisting of the bias voltages on the electrodes. Similar to the non-linear stiffness matrix, the capacitance matrix should be expressed in terms of analytical functions of the generalized coordinates, obtained either from analytical methods or by fitting capacitance data from BEM simulations.

These voltages define, together with the corresponding current terms I_{ij}, electrical interfaces of the marcomodel as required for the generalized Kirchoff equations. Hence the macromodel can easily be embedded into a electrical network simulator for system level simulation, combining the mechanical structure with the electronics. Due to the state depending capacitance matrix of the model, the capacitance currents I_{ij} have an additional term:

$$I_{ij} = C_{ij} \frac{d}{dt}(V_i - V_j) + \frac{dC_{ij}}{dt}(V_i - V_j) = C_{ij}(\dot{V}_i - \dot{V}_j) + (V_i - V_j)\sum_v \frac{\partial C_{ij}}{\partial q_v} \dot{q}_v$$

In most practical cases, in particular for switched capacitor implementations, the voltages applied to the electrodes are given and the electrical network is completely capacitive. Dynamics is only modeled in the mechanical part and the digital filtering operation of the electronic circuit, resulting in fast simulation times.

Returning to the general structures with flexible mechanical suspension as defined above, the kinetic energy T and potential energy E_{pot} are evaluated similarly. But an additional potential energy term has to be added to the two terms already discussed. The forces $F_{sus,i}$ at the suspension points are represented in the Largrange equations as the partial derivative of an external energy $E_{pot,ext}$ with respect to the corresponding suspension displacement $u_{sus,i}$. Since the forces as interface variables are needed in the systems equations, this energy is not needed to be evaluated.

$$F_{sus,i} = \frac{\partial E_{pot,ext}}{\partial u_{sus,i}} = \frac{\partial E_{pot,ext}}{\partial q_j} \quad with \quad q_j = u_{sus,i}$$

Again, the suspension force $F_{sus,i}$ and coressponding displacement $u_{sus,i}$ define a mechanical interface which enables the marcomodel to be introduced in a network simulator based on generalized Kichoff equations.

Setting up the Lagrange equations gives the marcomodel of the structure as a state space system with the generalized coordinates q_v and their derivatives $\dot{q}_v$ as state variables. The model has two sorts of interfaces: mechanical ones, described by force/displacement pairs, and electrical ones described by voltage/current pairs.

3. Free moveable plate

The technique above is applied to the structure shown in Fig. 1. As already mentioned, the two sets of eight fixed electrodes are used to sense capacitively the two tilting degrees of freedom and the vertical translation during the first half period of the sampling time T_S. Depending on the filtered sense signal, a voltage pattern of fixed amplitude is applied to the same electrodes for balancing the plate during the second half sampling period T_S. The applied voltage pattern is chosen to generate feedback forces at two fixed levels for each measured degree of freedom. As the feedback signal is quantized in time and amplitude, the system represents a typical Σ/Δ-modulator.

The used motion configuration of the moveable plate consists of the three rigid body motions which are detected and 4 eigenmodes, thus 7 generalized coordinates. These eigenmodes were obtained from a FEM model of the plate using ANSYS. Fig. 2. shows the two mode shapes related to the 1st and 3rd considered eigenmodes. The 2nd and 4th eigenmodes are the similar shapes, but rotated around the z-axis to give the respective orthogonal modes. These eigenmodes were primarily chosen, since the signal due to the 1st and 2nd eigenmodes is in first order orthogonal to the detection signal of the rigid body motions, while the signals due to the 3rd and 4th ones align with the 2 tilting degrees of freedom. The eigenfrequencies are 97.6 kHz and 225.3 kHz respectively. While determining the mode shapes the additional side-conditions for a free moveable object were set, i.e. the translation and rotation over the body volume are zero.

$$\int_V \vec{\mathbf{u}}(\vec{\mathbf{x}})dV = \vec{\mathbf{0}};\ \int_V \vec{\mathbf{x}} \times \vec{\mathbf{u}}(\vec{\mathbf{x}})dV = \vec{\mathbf{0}} \Rightarrow \int_V \vec{\mathbf{x}} \times \underline{\mathbf{G}} dV = \vec{\mathbf{0}}$$

Hence, the corresponding term in the expression for the kinetic energy disappears. Further, the thin, shell like form of the plate causes only displacements in the vertical direction during

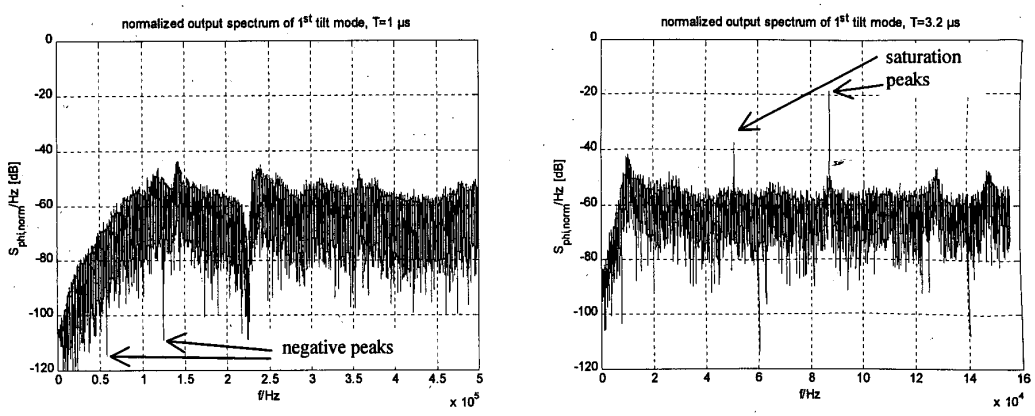

Fig. 3: normalized spectra of the output signal of the Σ/Δ-modulator with respect to the 1st tilt mode for a sampling time a.) $T_S = 1$ µs and b.) $T_S = 3.2$ µs

eigenmode analysis. As a consequence the complete matrix **A** in the expression for the kinetic energy vanishes. Similarly, all terms except two in the correction term for the matrix of moments of inertia evaluate to zero. The maximum relative modification of the matrix of moments of inertia due to these terms would be less than 1e-5. Therefore, they were neglected and the kinetic energy was finally retrieved from the matrix of moments of inertia of the undeformed structure and the mass matrix of the FEM model.

The inner potential energy was related to the stiffness matrix of the FEM model. For the electrical potential energy, the capacitances were calculated at 2187 points in the space, defined by the 7 generalized coordinates. The points lie within ±20% of the maximal possible amplitude, i.e. the plate touching the electrodes, with respect to each generalized variable separately. By interpolation with polynomial basis functions of this capacitance data the electrical energy was obtained.

Since the electrical network, which connected to the structure, ensures constant voltages at all electrodes (except a negligible settling time), only the capacitive network of the the structure itself has to be solved.

The structure was first simulated for sampling period T_S=1µs. While the spectrum of the vertical translation output signal was typically for a 2nd-order loop, the spectra with respect to the tilting modes is perturbed. This spectra of the 1st tilt mode, normalized to the square of the torque fed back, is shown in Fig. 3. Clearly, the negative tooth, due to the resonance of the 3rd and 4th eigenmode is visible. Since the detection signal of the vertical translation is orthogonal to all detection signals of the considered eigenmodes no such tooth affects the spectrum of the vertical translation. For similar reason, the 1st and 2nd eigenmodes aren't visible in the spectra of the tilt modes. The tooth indicates that the 3rd and 4th eigenmode is excited by the quantization noise. In this case the excitation is still small enough that the S/D-modulator doesn't overload.

In Fig. 3b the same spectrum is shown but with the sampling time extended to T_S=3.2µs. Here, the excitation of the 3rd and 4th eigenmode overlaods the S/D-loop, i.e. the quantization noise becomes correlated with the quantizer input. As an effect, strong peaks occur in the spectrum. Further, the baseband noise floor rises by about 20 dB, thereby lowering the signal to noise ratio by the same amount. This results demonstrates the significance to model eigenmodes of mechanical structures for S/D-loops, although this effect may be reduced by damping, which is not modeled here.

Further simulation results show effects due to small second order coupling. An applied signal, with respect to the vertical translation, occurred damped by 60 dB in the signal of the tilt modes. Fig. 3. shows strong negative peaks, which are likely to be folded version of the tooth due to non-linear effects.

4. Conclusion

The results above demonstrate that modern sense architectures used in micromechanical, multielectrode structures require verification of the inherent signal processing. For this verification, system level simulation is inevitable, but will only be effective if reduced models of the structures are used.

The described method to generate macromodels balances the need for sufficient model information to capture the major effects on the system inherent signal procesing with the required reduction of the model to ensure acceptable simulation times. Particularly, the consideration of eigenmodes of the structure in such macromodels has been shown as a requirement, since it influences significantly the behaviour of a Σ/Δ-modulator.

Realistic macromodels still require the inclusion of damping mechanisms and will be subject to further work.

[1] N.R. Swart, S.F. Bart, M.H. Zaman, M. Mariappan, J.R. Gilbert, and D.Murphy, *AutoMM: Automatic Generation of Dynamic Macromodels for MEMS Devices*, Proceedings MEMS 98, Heidelberg, Germany, 1998, pp. 178-83

[2] M. A. Lemkin, B. E. Boser, D. Auslander, J. H. Smith, *A 3-Axis Force Balanced Accelerometer Using a Single Proof-Mass*, Transducers '97. 1997 International Conference on Solid-State Sensors and Actuators, vol. 2, Chicago, 1997, pp. 1185-1188

[3] C.P. Lewis, M. Kraft, T.G. Hesketh, *Mathematical model for a micromachined accelerometer*, Trans. Inst. Meas. Control, vol. 18, no. 1, 1996, pp. 92-98

[4] S. D. Senturia, *CAD Challenges for Microsensors, Microactuators, and Microsystems*, Proceedings of the IEEE, vol. 86, no. 8, 1998, pp. 1611-26

[5] W. Greiner, *Mechanik Teil2* (Theoretische Physik, Band 2), 5 erw. Aufl., Verlag Harri Deutsch, Thun, Frankfurt am Main, 1989

[6] ANSYS Theory Reference, 3rd Edition, SAS IP,Inc.15.16 p.15-73